

[†]A NOVEL FORMULATION FOR DEFINING LINEARISING BASEBAND INJECTION SIGNALS OF RF POWER AMPLIFIER DEVICES UNDER ARBITRARY MODULATION

[†]F. L. Ogboi, [†]P.J. Tasker, [†]M. Akmal, [†]J. Lees, [†]J. Benedikt

[†]Centre for High Frequency Engineering, Cardiff University, Cardiff, United Kingdom,

^{*}S. Bensmida, ^{*}K. Morris, ^{*}M. Beach, ^{*}J. McGeehan

^{*}Centre for Communications Research, University of Bristol, Woodland Rd, Bristol, BS8 1UB, UK

[†]Email: ogboifl2@cardiff.ac.uk

Abstract — A new formulation, in the envelope domain for linearising RF power amplifier devices is demonstrated. By applying this formulation, it is possible to linearise RF power amplifiers by signal injection using a time varying baseband voltage signal. The formulation defines the baseband inter-modulation distortion (IMD) envelope as a function of the input carrier signal envelope. Irrespective of the modulated RF signal, intermodulation distortion envelopes can always be defined as a finite sum of distortion-envelopes multiplied by their control coefficients.

These coefficients are the keys used to optimise the time varying baseband voltage signal. In this formulation, ‘engineering’ the optimized time-varying baseband voltage signal requires the determination of only a finite number of constant coefficients. This eases the optimization process. This formulation was validated in an open-loop active baseband loadpull exercise on a 3-tone amplitude modulated RF signal. The investigation and validation experiment was performed on a Cree 10W GaN HEMT device, biased into class AB at 1.5 dB of compression. When the optimum linearizing baseband voltage was described, computed, engineered and injected into the device, IM3 and IM5 distortions were simultaneously suppressed for the optimum case to less than -56dBc. An improvement of 42dBc over the reference classical short circuit case.

Keywords — Multi-tone modulation, baseband, linearisation, non-linear distortion, envelope, power amplifier

I. INTRODUCTION

The degradation experienced in the linearity performance of wireless communication systems and their core devices is significantly attributable to the power amplifier transistor’s non-linear behavior. This is caused by the odd-order non-linearities generated by these devices in their active state. These odd order non-linearities are namely third, fifth, seventh, ninth but with the third and the fifth most disturbing. These in turn produce in-band inter-modulation distortions products, which occur very near the carrier frequencies of interest which makes them very difficult to remove by filtering. Various approaches have been suggested and used to try to suppress and minimize these distortion products ranging from feed-forward techniques, analog pre-distortion, digital pre-distortion and others [5-7].

In this paper we will focus on output baseband envelope voltage signal injection. It offers a simple technique aligned with the low cost requirement of small-cell transmitters, along with the prospect of combining with envelope tracking (ET) signals. We believe that this technique is a possible candidate to enable reduced DSP complexity in making the work of the pre-distorter easier. In addition, bandwidth is reduced when linearizing at baseband. The formulation is based on the basic principle of baseband injection which states that it is possible to utilize the transistor’s even order non-linearity to generate additional, ideally cancelling, in-band inter-modulation distortion. In this approach, the baseband specification is formulated not in terms of impedance, but in terms of the desired engineered envelope voltage signal. The importance is that it, allows the linearization solution to reduce to the determination of only a limited set of coefficients.

II. PRINCIPLE OF FORMULATION THEORY

Consider the behavior of a non-linear power transistor subjected to a modulated RF stimulus $V_{1,rf}(t)$ at its input, and a time-varying baseband stimulus $V_{2,bb}(t)$ at its output.

The arbitrary modulated input voltage signal can be represented and shown in Fig.1, as:

$$V_{1,rf}(t) = M_{1,rf}(t) \cos(\omega_c t + \phi_{1,rf}(t)) \quad (1)$$

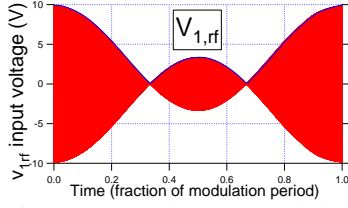


Fig 1. Measured 3-tone modulated RF input voltage signal plotted against time

where $M_{1,rf}(t)$ and $\phi_{1,rf}(t)$ are the magnitude and phase of the modulated input signal respectively, and ω_c is the RF carrier frequency.

This signal can also be presented mathematically in the complex envelope (I-Q) domain as:

$$\hat{V}_{1,rf}(t) = M_{1,rf}(t) \cos(\phi_{1,rf}(t)) - jM_{1,rf}(t) \sin(\phi_{1,rf}(t)) \quad (2)$$

Similarly, the RF output current response of the device can be represented and shown in Fig.2, as:

$$I_{2,rf}(t) = M_{2,rf}(t) \cos(\omega_c t + \phi_{2,rf}(t)) \quad (3)$$

where $M_{2,rf}(t)$ and $\phi_{2,rf}(t)$ are the magnitude and phase of the complex modulated output current respectively, and ω_c is the carrier frequency.

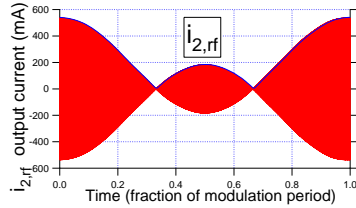


Fig.2. Measured 3-tone modulated RF output current signal plotted against time.

Again, this signal can be presented mathematically in the envelope domain, as:

$$\hat{I}_{2,rf}(t) = M_{2,rf}(t) \cos(\phi_{2,rf}(t)) - jM_{2,rf}(t) \sin(\phi_{2,rf}(t)) \quad (4)$$

Mixing analysis tells us that if $V_{2,bb}(t)=0$, the memory-less non-linear envelope transfer characteristic between the input voltage envelope $\hat{V}_{1,rf}(t)$ and the output current envelope $\hat{I}_{2,rf}(t)$ can be modeled as follows:

$$\hat{I}_{2,rf}(t) = \sum_{n=0}^m \alpha_{2n+1} |\hat{V}_{1,rf}(t)|^{2n} \hat{V}_{1,rf}(t) \quad (5)$$

where α_1 represents the linear gain of the system, α_3 quantifies the level of third order intermodulation distortion, α_5 quantifies the level of fifth order intermodulation distortion, and so on, up to the desired maximum order m .

In this work, the following general envelope formulation for the output baseband voltage envelope signal $\hat{V}_{2,bb}(t)$ is considered:

$$\hat{V}_{2,bb}(t) = \sum_{p=1}^q \beta_{2p} |\hat{V}_{1,rf}(t)|^{2p} \quad (6)$$

where β_{2p} is the even order voltage component scaling coefficient and q specifies the desired maximum range. The motivation for using this formulation lies in the fact that only cancelling odd-order intermodulation terms will be added to the RF output current envelope response. Hence, only the coefficients in equation (5) will be modified such that

$$\alpha_{2n+1} |_{n=1}^m = f(\beta_2, \beta_4, \dots, \beta_{2p}, \dots, \beta_{2q}) \quad (7)$$

Consider now a system with intermodulation distortion up to fifth order ($m=2$). The baseband linearization problem can now be restricted to fourth order ($q=2$), hence equating to determining the values of β_2 (beta-2) and β_4 (beta-4) that can simultaneously satisfy the two following conditions:

$$\alpha_3 = f(\beta_2, \beta_4) = 0$$

$$\alpha_5 = g(\beta_2, \beta_4) = 0$$

(8)

and where f and g are unknown generic functions, to be determined empirically.

III. ENVELOPE MEASUREMENT SYSTEM

To investigate this concept, the Large Signal Waveform Measurement System (LSWMS) described in [8], shown in Fig. 3, capable of measuring modulated voltage and current waveforms while also injecting voltage signals into the baseband, was modified to support the formulation and utilized. The major modification shown in red in Fig. 3 and further described in Fig. 6 was made to ensure that the appropriate output baseband envelope voltage signal can be generated. In addition, the system was further enhanced by the addition of a 75W, 10 KHz-250MHz wideband baseband amplifier from “Amplifier Research” Model 75A250. Key to this system enhancement is an ability to describe, compute, measure, engineer and inject the modulated time domain terminal voltage and current envelope waveforms. Using this information, it is possible to compute all the necessary measured envelope stimulus components at both baseband and RF (fundamental and harmonics).

The LSWMS was calibrated to the device package plane using a custom built 50 Ω TRL test fixture, over a 50MHz baseband bandwidth and over a 100 MHz bandwidth around each of the RF components (fundamental and harmonics). Using a 1 MHz 3-tone, modulated excitation signal with peak-to-average power ratio (PAPR) of 4.77dB and centered at 2GHz, the GaN device was biased in class AB, with RF fundamental and all harmonic frequencies terminated into a passive 50 Ω .

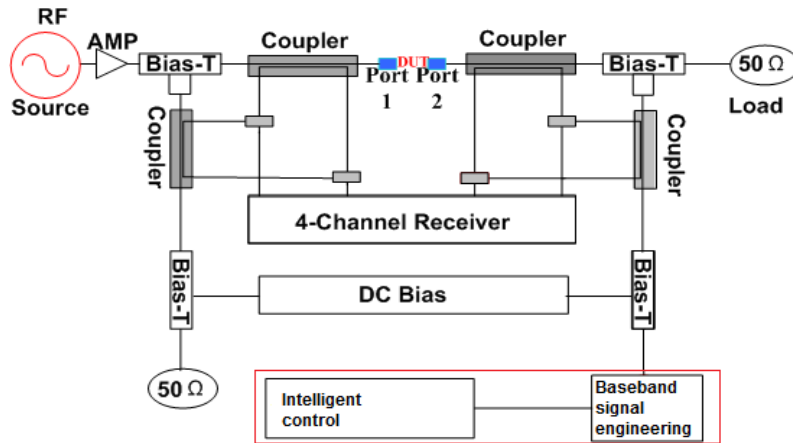


Fig. 3. Large signal modulated RF waveform measurement system.

Drain and gate bias voltages were +28V and -2.8V respectively, giving a quiescent drain current of approximately 20% I_{DSS} . The load condition, although not quite optimal, was considered sufficiently close for this demonstration. Typical measured fundamental input voltage $\hat{V}_{1,rf}(t)$ and output current $\hat{I}_{1,rf}(t)$ complex envelopes are shown in Fig. 4. These use polar form (magnitude and phase), and indicate a clear AM-AM distortion, but only a very weak AM-PM distortion of less than +/- 2 degrees.

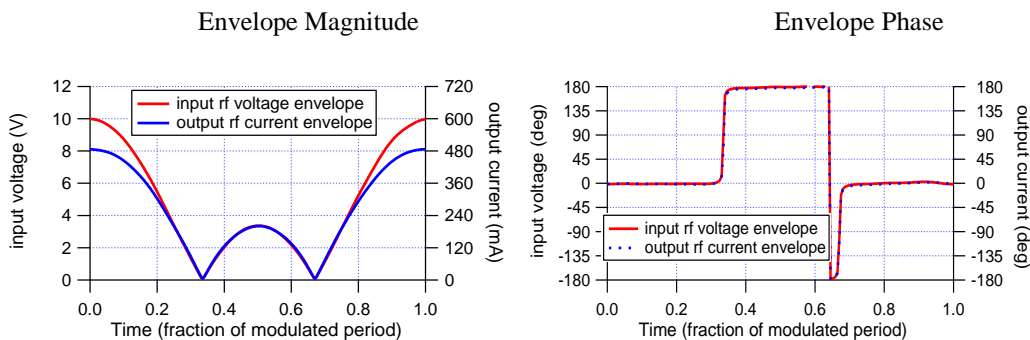


Fig. 4. Measured magnitude and phase of the time aligned fundamental input voltage $\hat{V}_{1,rf}(t)$ and output current $\hat{I}_{1,rf}(t)$ envelopes.

Fig. 5, however shows the measured transfer magnitude and phase of the fundamental input voltage $\hat{V}_{1,rf}(t)$ at the baseband short circuit reference state. These also confirm the presence of AM/AM distortion and minimal AM/PM distortion.

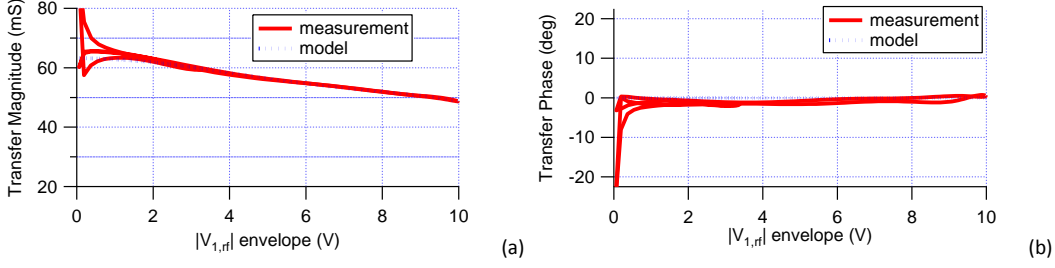


Fig. 5. Measured transfer magnitude (a) and phase (b) of the fundamental input voltage $\hat{V}_{1,rf}(t)$ envelope at the reference baseband short circuit state.

IV. ENVELOPE SIGNAL ENGINEERING

For the measurements shown in Fig. 4, the system was configured to force the baseband output voltage component $V_{2,bb}(t)$ to zero, hence $\beta_2 = 0$ and $\beta_4 = 0$. Since the measured baseband output current $I_{2,bb}(t)$ is observed to vary when the baseband output voltage $V_{2,bb}(t)$ is modified, an intelligent, iterative software control loop was needed to ‘engineer’ the targeted baseband output voltage. This intelligent control loop, is modeled using the circuit representation shown in Fig. 6. It depicts the behavior of the baseband injection system, which is a major modification to the LSWMS. This causes a systematic but scientific iterative waveform-engineering process to occur as the baseband voltage waveform is shaped by the linearising coefficients in each new iteration according to a mathematical model. This process was used to engineer the low frequency signals in the baseband (DC) region to target intermodulation distortion envelopes, as depicted in the spectral map in Fig.7.

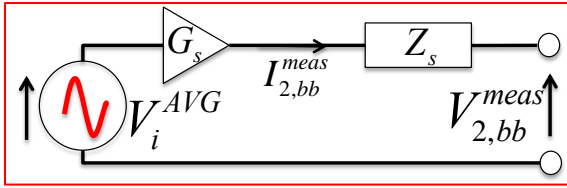


Fig. 6. Circuit Model for baseband voltage engineering.

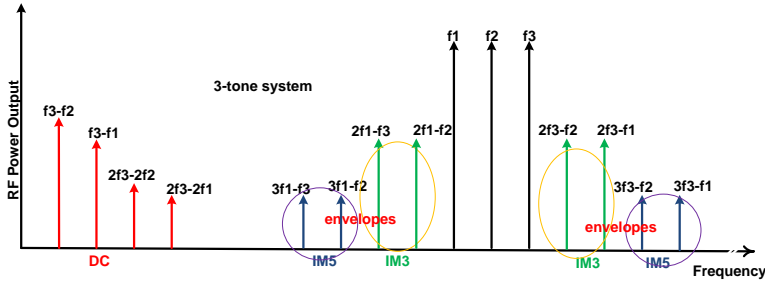


Fig. 7. Spectral map showing intermodulation distortion envelopes.

Initially, the system is calibrated to determine the values of natural system impedance $Z_s(\omega)$ and load-pull loop gain $G_s(\omega)$, over the desired modulation bandwidth (in this case 5 MHz). An iterative process using equation 9 is used to synthesize exactly the desired baseband voltage waveform $V_{2,bb}^{target}(t)$. The measured values of baseband voltage $V_{2,bb}^{meas,i}(t)$ and current $I_{2,bb}^{meas,i}(t)$ at iteration i , are transformed into frequency domain baseband voltage $\hat{V}_{2,bb}^{meas,i}(\omega)$ and current $\hat{I}_{2,bb}^{meas,i}(\omega)$, and are then used to compute a new baseband voltage requirement at iteration $i+1$, also formulated in the frequency domain, using the following equation;

$$V_{i+1}^{avg}(\omega) = (1 - w)V_i^{avg}(\omega) + w \left(\frac{V_{2,bb}^{target}(\omega) - Z_s(\omega)I_{2,bb}^{meas,i}(\omega)}{G_s(\omega)} \right) \quad (9)$$

where w is the static weighting factor. This process is repeated until the desired output baseband target voltage waveform is achieved, within a specified error limit. Typically, when the desired error limit is set to 1mV, the system converges to the desired baseband voltage within 5-6 iterations.

V. FORMULATION APPLICATION

To quantify the level of observed distortion, the measured fundamental envelope transfer function (fundamental RF output current envelope $\hat{I}_{2,rf}(t)$ plotted against the fundamental RF input voltage envelope $\hat{V}_{1,rf}(t)$) was time aligned to remove the effect of linear delay, and then analyzed. A least-squares curve fitting approach was used to fit the model, given by equation (5), to the measured envelope transfer characteristic, and hence determine the coefficients α_1 , α_3 and α_5 for each case. A typical comparison of the measured and modeled envelope transfer function; $|\hat{I}_{2,rf}(t)|$ versus $|\hat{V}_{1,rf}(t)|$ is shown in Fig. 8. The results in this case also confirm that the DUT has very little observable memory.

Fig. 8 shows the resulting spectral contributions of each component generated by the current model. The labels shown on the spectral graph are the corresponding computed output power levels. The maximum power level of the out-of-band distortion, in this un-linearised 1.5 dB compressed case, can be seen to be -12 dBc. Note this is the result obtained when $\beta_2 = 0$ and $\beta_4 = 0$, the reference baseband short circuit case.

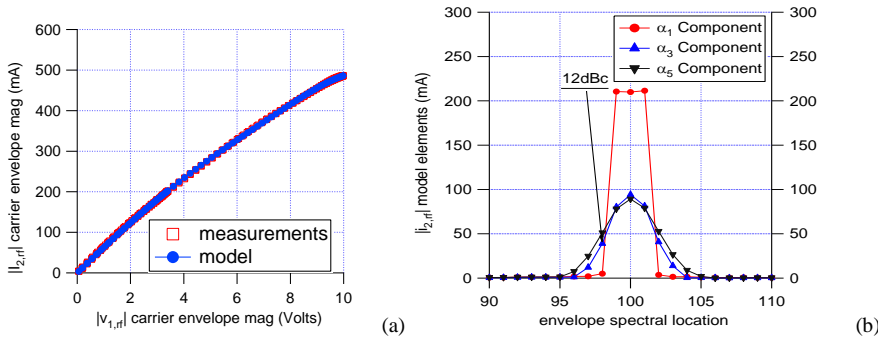


Fig 8. Comparison of the measured and modeled envelope transfer (a) function for the case $V_{2,bb}(t) = 0$. Also shown is the spectral contribution (b) of the individual model components, $\alpha_3 = -0.2$, $\alpha_5 = 0.0008$

To investigate how effective precisely engineered baseband voltages can be in linearizing the device, a sequence of measurements was performed; sweeping the baseband voltage waveform describing coefficients β_2 and β_4 over a selected range, thus systematically varying the injected voltage waveform. The variation of the level of observed distortion in the measured fundamental transfer characteristic was then determined. The measured observed variations of the third order distortion term α_3 and fifth order distortion term α_5 , were plotted as various contours plots as shown in Fig. 9 – 12.

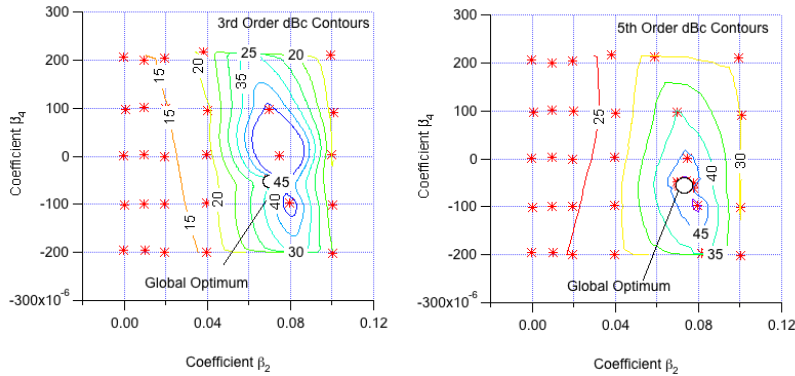


Fig 9. Contour plots of measured third order term α_3 and fifth order term α_5 values as a function of swept β_2 and β_4 .

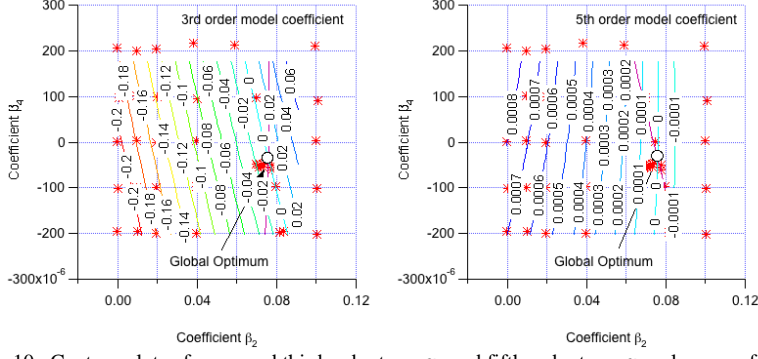


Fig 10. Contour plots of measured third order term α_3 and fifth order term α_5 values as a function of swept β_2 and β_4 .

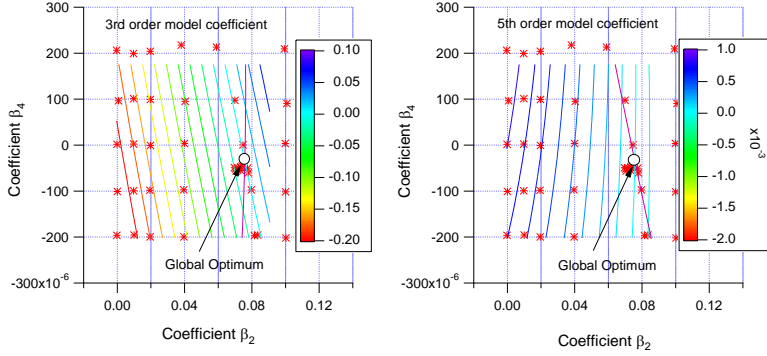


Fig 11. Contour plots of measured third order term α_3 and fifth order term α_5 values as a function of swept β_2 and β_4 .

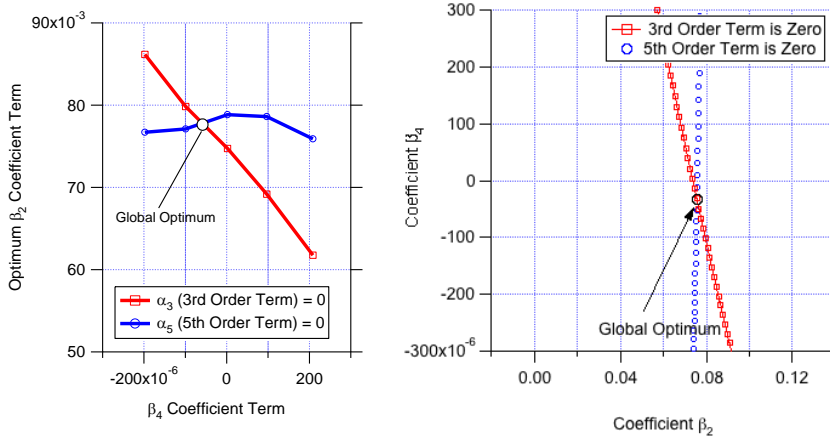


Fig 12. Contour plots of measured third order term α_3 and fifth order term α_5 values as a function of swept β_2 and β_4 .

The contour plots in Fig. 9 show the level of suppression, Fig. 10 show the values of the linearizing coefficients around the suppression levels and Fig. 11 show a unified contour-point plot for clarity. All three plots indicate that there is an optimum set of values for β_2 and β_4 that can simultaneously satisfy the condition $\alpha_3 = 0$ and the condition $\alpha_5 = 0$. Fig. 12 however, shows the global optimum-point where simultaneous suppression occurs. In other words, there is a baseband voltage waveform, that when injected into the device output, will linearize the device.

VI. LINEARISED PERFORMANCE

The measurement system was now configured to demonstrate engineered baseband linearization. Using the optimum values determined above, the required ‘linearizing’ output baseband voltage was computed using equation (6). This computed target waveform along with the measured output baseband voltage waveform achieved are shown in Fig 13, indicating the ability of the system to correctly identify and engineer the required

baseband voltage signal. The corresponding measured value of the baseband current $I_{2,bb}(t)$ defined by equation (10) is also shown. Note, the current and voltage variations are in phase, indicating that this condition would in practice require an active envelope tracking (ET) type of drain bias. This is interesting as it raises the possibility of improving efficiency and linearity simultaneously [9]. The ‘zoom-in’ plot also show, that the measured and the target time varying baseband voltage $V_{2,bb}(t)$ have considerable agreement. Secondly, that the measured baseband current $I_{2,bb}(t)$ has maintained the same form as the agreeing voltages.

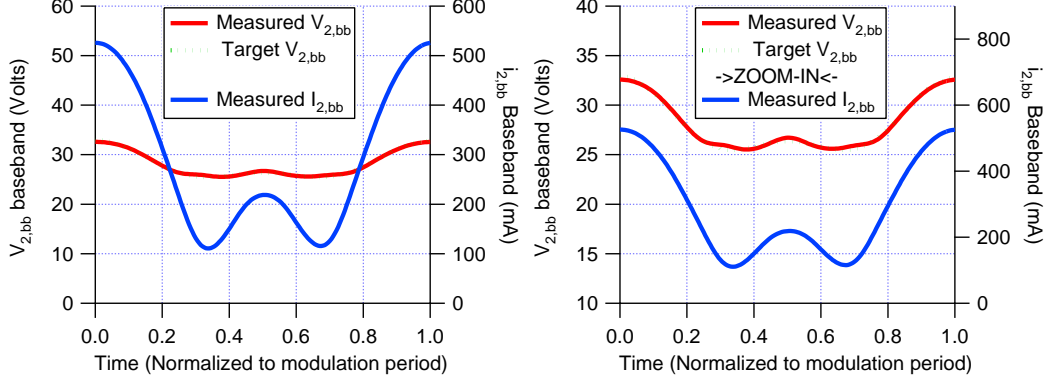


Fig. 13. Measured baseband output current (blue), ideal (green) and measured (red) optimum output baseband linearizing voltage waveform and depicting ET type formation.

$$I_{2,bb}(t) = \sum_{n=1}^m \alpha_{2n} |\hat{V}_{1,rf}(t)|^{2n} \quad (10)$$

The linearizing baseband voltage signal was applied and the resulting, now linear transfer characteristic is shown in Fig. 14. Again the spectral contribution of each component generated by the current model obtained in this state is also shown.

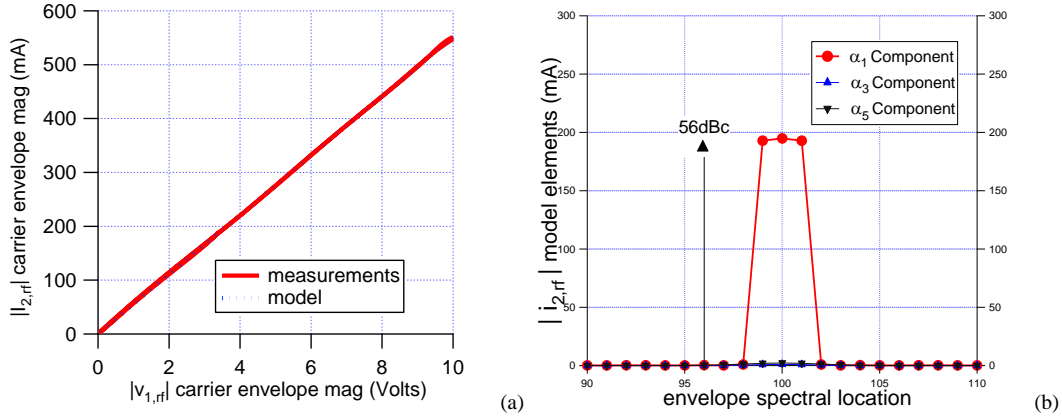


Fig. 14. Comparison of the measured and modeled envelope transfer function (a), for the optimum $V_{2,bb}(t)$ case. Also shown is the spectral contribution (b), of the individual model components. $\alpha_3 = \alpha_5 = 0$, $\beta_2 = 0.076$, $\beta_4 = -0.000033$

In this case both the third order and fifth order IMD contributions are now reduced to below -56dBc, which is an improvement of 42dBc over the reference, baseband short circuit solution. The actual measured input and output power spectra around the carrier are shown in Fig. 15.

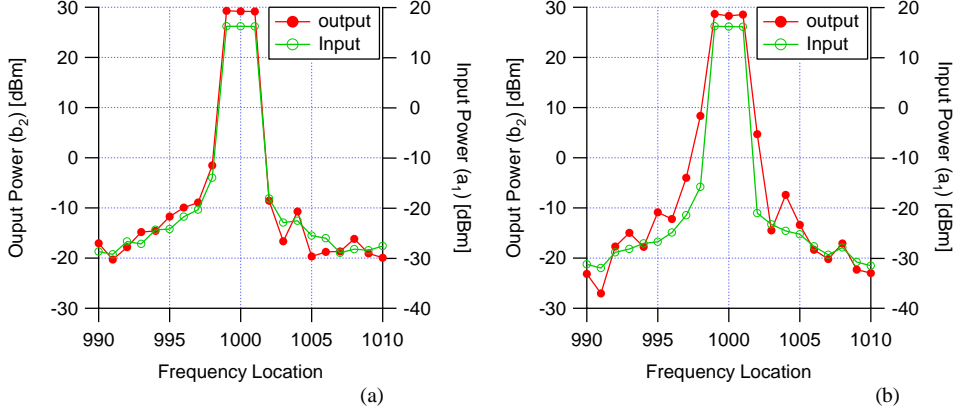


Fig. 15. Measured input and output power spectra around the carrier at linear (a) and baseband short circuit (b) states.

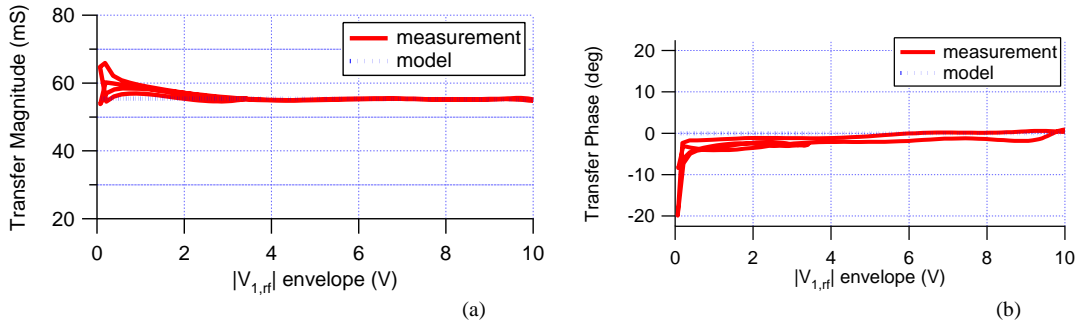


Fig. 16. Measured transfer magnitude (a) and phase (b) of the fundamental input voltage $\tilde{V}_{1,rf}(t)$ envelope at the linear state.

It is important to realize that the plot in Fig. 15 shows that the modulated excitation being used to excite the device is certainly not perfect, and contains significant distortion, mostly due to the driver amplifier being used. As both axis cover 60dB dynamic range, it is still effective in showing however that no detectable, additional distortion is being introduced by the baseband linearized device. Shown in Fig. 16 are the plots of the measured transfer magnitude and phase of $\tilde{V}_{1,rf}(t)$ envelope at the linear state also showing considerable linearity.

VII. CONCLUSION

A formulation and technique for defining linearising baseband injection signals of RFPA devices under arbitrary modulation in the AM/AM environment, with the ability to enable automatic engineering of specific baseband voltages, that when injected into the output port of a device causing the device to linearise has been demonstrated.

This functionality is achieved using a formulation, generalized in the envelope domain, which can be used to describe the required “linearizing” baseband injection signal, for an arbitrary amplitude modulated envelope, using a limited set of coefficients. The ability of the approach to simultaneously minimize both third and fifth order distortion terms was demonstrated using a 3-tone modulated signal, where the optimum baseband signal voltage for third and fifth order IMD suppression was successfully determined and then used to linearize the device.

This knowledge can be useful in the design of amplifier bias network at baseband frequency on device performance. As at the time of this submission, this approach has been successfully applied to further linearise, a 3-tone, 5-tone and 9-tone modulation. In addition, it has been used to linearise a modulation bandwidth of 20MHz on a 3-tone system in steps of 2MHz. It has also been used to linearise a HV-LDMOS, GaAs and Nitronex devices. Hence we believe it can be applied to both arbitrary modulation and arbitrary modulation bandwidth and arbitrary RFPA device.

Further work is now planned to use this system to show that this approach can be applied to AM/PM environment and subsequently used in a real base-station network.

ACKNOWLEDGEMENT

This work is supported by EPSRC (grant EP/F033702/1). We also thank CREE for supplying devices and specifically Simon Wood, Ryan Baker and Ray Pengelly.

REFERENCES

- [1] Andrei Grebennikov, "RF and Microwave Power Amplifier Design". McGraw-Hill ISBN 0-07-144493-9
- [2] Joel Vuolevi and Timo Rahkonen, "Distortion in RF Power Amplifiers", Norwood, MA: Artech House, 2003.
- [3] John Wood, David E. Root, "Fundamentals of nonlinear behavioral modeling for RF and microwave design". Artech House, 2005.
- [4] J. C. Pedro, N. B. Carvalho, "Intermodulation Distortion in Microwave and Wireless Circuits" Artech House, 2003.
- [5] Chi-Shuen Leung, Kwok-Keung, M. Cheng, "A new approach to amplifier linearization by the generalized baseband signal injection method," *IEEE microwave and wireless components letters*, vol. 12, no.9, September, 2002.
- [6] Lei Ding, G. Tong Zhou. "Effects of Even-Order Nonlinear Terms on Power Amplifier Modelling and Predistortion Linearization". *IEEE Transactions On Vehicular Technology*, Vol. 53, No. 1, January 2004.
- [7] Vincent W. Leung, Junxiong Deng, Prasad S. Gudem, and Lawrence E. Larson. "Analysis of Envelope Signal Injection for Improvement of RF Amplifier Intermodulation Distortion", *IEEE Journal of solid-state circuits*, vol. 40, no. 9, September 2005
- [8] Akmal, M.; Lees, J.; Jiangtao, S.; Carrubba, V.; Yusoff, Z.; Woodington, S.; Benedikt, J.; Tasker, P.J.; Bensmida, S.; Morris, K.; Beach, M.; McGeehan, J., "An enhanced modulated waveform measurement system for the robust characterization of microwave devices under modulated excitation," *Microwave Integrated Circuits Conference (EuMIC), 2011 European*, vol., no., pp.180,183, 10-11 Oct. 2011
- [9] Akmal, M.; Carrubba, V.; Lees, J.; Bensmida, S.; Benedikt, J.; Morris, K.; Beach, M.; McGeehan, J.; Tasker, P.J., "Linearity enhancement of GaN HEMTs under complex modulated excitation by optimizing the baseband impedance environment," *Microwave Symposium Digest (MTT), 2011 IEEE MTT-S International*, vol., no., pp.1,4, 5-10 June 2011. doi: 10.1109/MWSYM.2011.5972833
- [10] Akmal, M.; Ogboi, F.L.; Yusoff, Z.; Lees, J.; Carrubba, V.; Choi, H.; Bensmida, S.; Morris, K.; Beach, M.; McGeehan, J.; Benedikt, J.; Tasker, P.J., "Characterization of electrical memory effects for complex multi-tone excitations using broadband active baseband load-pull," *Microwave Conference (EuMC), 2012 42nd European*, vol., no., pp.1265,1268, Oct. 29 2012-Nov. 1 2012
- [11] Akmal, M.; Lees, J.; Bensmida, S.; Woodington, S.; Carrubba, V.; Cripps, S.; Benedikt, J.; Morris, K.; Beach, M.; McGeehan, J.; Tasker, P.J., "The effect of baseband impedance termination on the linearity of GaN HEMTs," *Microwave Conference (EuMC), 2010 European*, vol., no., pp.1046,1049, 28-30 Sept. 2010
- [12] Akmal, M.; Lees, J.; Bensmida, S.; Woodington, S.; Benedikt, J.; Morris, K.; Beach, M.; McGeehan, J.; Tasker, P.J., "The impact of baseband electrical memory effects on the dynamic transfer characteristics of microwave power transistors," *Integrated Nonlinear Microwave and Millimeter-Wave Circuits (INMMIC), 2010 Workshop on*, vol., no., pp.148,151, 26-27 April 2010 doi: 10.1109/INMMIC.2010.5480111
- [13] Akmal, M.; Lees, J.; Carrubba, V.; Bensmida, S.; Woodington, S.; Benedikt, J.; Morris, K.; Beach, M.; McGeehan, J.; Tasker, P.J., "Minimization of baseband electrical memory effects in GaN HEMTs using active IF load-pull," *Microwave Conference Proceedings (APMC), 2010 Asia-Pacific*, vol., no., pp.5,8, 7-10 Dec. 2010
- [14] Benedikt, J.; Tasker, P.J., "High-power time-domain measurement bench for power amplifier development," *ARFTG Conference Digest, Fall2002.60th*, vol., no., pp.107,110,5-6 Dec.2002, doi: 10.1109/ARFTGF.2002.1218692
- [15] Lees, J.; Akmal, M.; Bensmida, S.; Woodington, S.; Cripps, S.; Benedikt, J.; Morris, K.; Beach, M.; McGeehan, J.; Tasker, P., "Waveform engineering applied to linear-efficient PA design," *Wireless and Microwave Technology Conference (WAMICON), 2010 IEEE 11th Annual*, vol., no., pp.1,5,12-13 April 2010 doi: 10.1109/WAMICON.2010.5461847
- [16] Lees, J.; Williams, T.; Woodington, S.; McGovern, P.; Cripps, S.; Benedikt, J.; Tasker, P., "Demystifying Device related Memory Effects using Waveform Engineering and Envelope Domain Analysis," *Microwave Conference, 2008. EuMC 2008. 38th European*, vol., no., pp.753,756,27-31 Oct.2008 doi: 10.1109/EUMC.2008.4751562
- [17] Ogboi, F.L.; Tasker, P.J.; Akmal, M.; Lees, J.; Benedikt, J.; Bensmida, S.; Morris, K.; Beach, M.; McGeehan, J., "A LSNA configured to perform baseband engineering for device linearity investigations under modulated excitations," *Microwave Conference (EuMC), 2013 European*, vol., no., pp.684,687, 6-10 Oct. 2013
- [18] Tasker, P.J., "RF Waveform Measurement and Engineering," *Compound Semiconductor Integrated Circuit Symposium, 2009. CISC 2009. Annual IEEE* vol., no., pp.1,4,11-14 Oct.2009 doi: 10.1109/csics.2009.5315818
- [19] Tasker, P.J., "Practical waveform engineering," *Microwave Magazine, IEEE*, vol.10, no.7, pp.65,76, Dec.2009 doi: 10.1109/MMM.2009.934518
- [20] Tasker, P.J., "Non-linear characterisation of microwave devices," *High Performance Electron Devices for Microwave and Optoelectronic Applications, 1999. EDMO. 1999 Symposium on*, vol., no., pp.147,152, 1999 doi: 10.1109/EDMO.1999.821476
- [21] Tasker, P.J.; Reinert, W.; Braunstein, J.; Schlechtweg, M., "Direct Extraction of All Four Transistor Noise Parameters from a Single Noise Figure Measurement," *Microwave Conference, 1992. 22nd European*, vol.1, no., pp.157,162, 5-9 Sept. 1992 doi: 10.1109/EUMA.1992.335733
- [22] Williams, D.J.; Leckey, J.; Tasker, P.J., "Envelope domain analysis of measured time domain voltage and current waveforms provide for improved understanding of factors effecting linearity," *Microwave Symposium Digest, 2003 IEEE MTT-S International*, vol.2, no., pp.1411,1414 vol.2, 8-13 June 2003 doi: 10.1109/MWSYM.2003.1212636
- [23] Williams, D.J.; Leckey, J.; Tasker, P.J., "A study of the effect of envelope impedance on intermodulation asymmetry using a two-tone time domain measurement system," *Microwave Symposium Digest, 2002 IEEE MTT-S International*, vol.3, no., pp.1841,1844 vol.3, 2-7 June 2002 doi: 10.1109/MWSYM.2002.1012221
- [24] Williams, D.; Tasker, P.J., "Thermal parameter extraction technique using DC I-V data for HBT transistors," *High Frequency Postgraduate Student Colloquium, 2000*, vol., no., pp.71,75, 2000 doi: 10.1109/HFPSC.2000.874085
- [25] Williams, D.J.; Tasker, P.J., "An automated active source and load pull measurement system," *High Frequency Postgraduate Student Colloquium, 2001. 6th IEEE*, vol., no., pp.7,12, 2001 doi: 10.1109/HFPSC.2001.962150

- [26] Z. Yusoff, J. Lees, J. Benedikt, P.J. Tasker, S.C. Cripps, "Linearity improvement in RF power amplifier system using integrated Auxiliary Envelope Tracking system," *IEEE MTT-S Int. Microw. Symp. Dig.*, 2011, vol., no., pp.1-4, 5-10 June 2011.